Available online at www.sciencedirect.com
ScienceDirect
Solar Energy 84 (2010) 401–408
SOLAR ENERGY
www.elsevier.com/locate/solener

Lifetime and recombination kinetics in a-Se thin films

R. Kaplan *

Department of Secondary Science and Mathematics Education, University of Mersin, Yenisehir Campus, 33169 Mersin, Turkey

Received 25 August 2009; received in revised form 10 December 2009; accepted 16 December 2009
Available online 12 January 2010

Communicated by: Associate Editor Takhir Razykov

Abstract

Modulated photoconductivity measurements in amorphous selenium (a-Se) thin films were carried out. Especially, photocarrier lifetime as a function of applied electric field (d.c.) and temperature was determined by using the quadrature frequency-resolved spectroscopy (QFRS) method. At low temperature, two different carrier lifetime channels were observed. However, only one carrier lifetime channel was dominated at room temperature (297 K). The temperature dependence of the frequency-resolved photocurrent (FRPC) was investigated under different applied electric fields. At high temperatures, a small field independent activation energy value of 147 ± 35 meV was determined, in which hole transport is controlled by the valence band-tail states. The exponent v in the power-law relationship ($I_{ph} \propto G^{v}$) between generating flux and photocurrent was obtained at different electric fields and excitation wavelengths. The value of v increases very little with decreasing applied electric fields. However, v shows a little stronger dependence on the excitation wavelengths. The applied electric field dependences of photocurrent at different excitation wavelengths were also directly measured. However, a little non-ohmic behaviour was observed at high applied electric fields and at low excitation wavelengths measured. We explained it in the frame of traditional models.

Keywords: Amorphous selenium; Photocurrent; Lifetime; Recombination; Trapping

1. Introduction

Since 1980 amorphous semiconductors have become increasingly important because of their applications in modern technology. The technological uses of these semiconductors can be roughly divided into two classes (Joraid et al., 2008): (i) hydrogenated amorphous silicon (a-Si:H) type alloys (Green, 2003, 2004; Goswami et al., 2004; Waldau, 2004; Lee, 2009; Acevedo, 2009), whose applications include photovoltaic solar cells, thin film transistors, image scanners, electrophotography, optical recording and sensors; and (ii) amorphous chalcogenide glasses (Kessler and Rudmann, 2004; Bhattacharya and Ramanathan, 2004; Gorley et al., 2008), whose applications include: switching, electrophotography and memory devices. Recently, promising new applications of chalcogenide materials have occurred in the fields of infrared spectroscopy, laser and fiber techniques (Sharma et al., 2008). Amorphous selenium (a-Se) thin film and its compounds continue to be of great interest (Pawar et al., 2007; Bindu et al., 2002; Hayashi and Mitsuishi, 2002; Zhang and Drabold, 1998; Petretis and Balciuniene, 1998; Shirakawa et al., 2002; Li et al., 2006; Venkatachalam et al., 2009). They play a crucial role in the present day science and modern technology due to their wide use in a large number of active and passive devices (Kolobov and Tanaka, 2001).

The common feature of chalcogenide glassy semiconductors is the presence of localized states in the mobility gap due to the absence of long range order as well as inherent defects. Photocurrent measurements have been widely used for understanding the defect states in these materials (Thakur et al., 2006; Murugvel and Asokan, 2002). Recom-

* Tel.: +90 324 3412815; fax: +90 324 3412823.
E-mail address: ruhikaplan@yahoo.com

0038-092X/$ - see front matter © 2009 Elsevier Ltd. All rights reserved.
doi:10.1016/j.solener.2009.12.010

bination is a key feature when describing carrier transport in chalcogenide semiconductors because it strongly affects the photoresponse of these semiconductors at all levels of external excitation. The study of frequency-resolved photocurrent (FRPC) as a function of temperature, applied electric field, excitation wavelength and intensity is a valuable tool in achieving a good understanding of the recombination processes and distribution of localized states which control the FRPC kinetics (Dahson et al., 2006; Emelianova et al., 2003; Lyubin et al., 2002; Petretis and Balciuniene, 2002; Nesheva, 1996; Kaplan, 1993; Mellor et al., 2009). However, in spite of the extensive studies, the interpretation of experimental data still remains difficult.

In this work, we determined the photocarrier lifetime, the exponent v in the power-law relationship $I_{ph} \propto G^v$, and their dependences on the applied electric field, temperature and excitation wavelength for a-Se. We also attempted to interpret our experimental results in the frame of predictions of photoconductivity models proposed.

2. Experimental

The samples of a-Se were a thin film prepared by standard thermal vacuum evaporation. The material used for these samples was from BDH chemicals with a purity of 99.9992%. During the thermal evaporation of the films, the work chamber pressure was less than 10^{-6} Torr. The substrates (Corning 7059 glass) were held at room temperature (290 K). The thicknesses of samples were of the order of 1 μm. Au or Al contacts were then evaporated on the film in a coplanar configuration. The spacing between the contacts was 0.13 mm. Copper wires were placed on Au or Al layers with electrically conductive silver paint.

The sample was excited by a HeNe or Ar^+ dye laser. An acousto-optic modulator (IntraAction Corp., Model AOM-125) was used to modulate the light sinusoidally in the frequency range of 10 Hz to 100 kHz. The modulation amplitude amounted to 46% of the bias light intensity. The modulated photocurrent signal excited in this way was measured and analysed by a lock-in amplifier (SR 530 Stanford Research System). During the measurements the sample was kept in a helium exchange-gas cryostat in which the temperature could be varied between room temperature and 20 K. The vacuum pressure of the cryostat was about 10^{-6} Torr. Light intensities were varied by using a set of neutral density filters.

The lifetime of the photocurrent was studied by means of frequency-resolved spectroscopy (FRS) in which the in-phase and out-of-phase components of the photocurrent signal were obtained from the lock-in amplifier. The lifetime distribution was obtained from the out-of-phase signal. The intensity of the out-of-phase signal is approximately proportional to the lifetime distribution at $\tau = \frac{1}{2\pi f}$ where τ denotes the lifetime. However, the lifetime distribution of the electron–hole pairs is broad and featureless. The FRS method will be discussed in next sections.

3. Analysis of lifetime distributions

Lifetime analysis can be carried out by making measurements in the time domain (Time-Resolved Spectroscopy, TRS) or in the frequency domain (Frequency-Resolved Spectroscopy, FRS). In principle they are equivalent and contain the same information (related by a Fourier transform), granted they are done under the same excitation conditions. For example, the build up of a metastable population, which tends to occur with a long exposures experienced used in a FRS exponent are not necessarily produced with a single excitation pulse. Their comparative advantages and disadvantages was clearly given by Searle (1991), though in a discussion of photoluminescence (PL). TRS uses a δ-function (in time) excitation pulse and follows the response in time, while the FRS uses a sinusoidal excitation (δ-function in frequency) and follows the (complex) response in frequency. For FRS, the modulation is most conveniently produced with an Acousto-Optic-Modulator (AOM), and the signal recovered with a phase sensitive detector such as lock-in amplifier. It turns out that the quadrature response alone closely resembles a broadened lifetime distributions: the Fourier transform of a single well defined lifetime, which yields a single exponential in time domain, produces a Lorentzian just under a decade wide in the quadrature frequency domain. The quadrature method is therefore not well studied to materials exhibiting only one or two decay times, but loses little information where lifetime distributions are continuous and slowly varying.

Both TRS and FRS methods have a role and have been used, particular for PL, in a-Si:H and chalcogenide glasses. Fast processes are most easily studied in the time domain, for commercially available lock-in amplifiers have a bandwidth less than 200 kHz, limiting the quadrature methods to lifetimes longer than $1/(2\pi 2 \times 10^5) \approx 800$ ns. In contrast, many pulsed lasers have pulsewidths less than 10 ns, and long (20 ns and upward) but sharp edged pulses (10 s) can easily be sliced out of a CW laser. With digital CRO or multichannel analysers decays on this timescale can be easily recovered so long as the signal is large (mV), and digital averaging avoids some of the restrictions of the low repetition rate of some pulsed lasers. When the material contains a wide range of lifetimes it is usual with the sliced pulse method to join together the response to a set of pulses of increasing length (Tsang and Street, 1979). This works well as long as the excitation intensity is unchanged and not increased to enhance the weaker long time signal.

For the slower parts of the lifetime distribution the quadrature technique has a number of advantages. First, excitation conditions are well defined and frequency independent: in particular, the excitation intensity is constant, making it straight-forward to investigate intensity dependence of the distribution. Second, these excitation conditions are the same as used to measure (in-phase) PC efficiencies, or in the limit of zero frequency (d.c.) the total PC efficiency η. Third, the method can be easily modified to examine the kinetics under small signal conditions, which

may ease the analysis, or to look at the effects of a steady background of electron–hole pairs. One can, for example easily use the zero order beam from the modulator rather than the first order beam with its almost true intensity zeros.

The experimental aspect of the method which requires the most care is keeping exactly in-quadrature as the frequency is swept: one approach is to obtain a phase correction versus frequency correction curve for a particular detector–amplifier combination. This correction can then be held by the same computer which controls the frequency (via the voltage controlled oscillator) and used to correct the phase through an external phase input to the lock-in during the sweep. The quadrature signal is, of course much more sensitive to phase inaccuracies than the in-phase for small ϕ.

We used FRS method to measure the lifetime distributions of a-Se. All of our lifetime measurements and data storages are fully computer controlled. The acousto-optic device driven by a sinewave voltage signal provides the laser modulation in the system, the magnitude of the voltage signal ($16V_{pp}$ in our case) determines the modulation depth and thus the value of modulated component (F_m) of excitation intensity. The maximum value of F_m available for HeNe laser light is about 46%. However, the voltage magnitude bigger than $16V_{pp}$ causes the modulation depth to saturate. This can be easily examined on the CRO by using Si detector. It should be noted that the modulation depth has no important influence on our PC results.

The mathematical analysis of FRS method has already been described by Depinna et al. for PL (Depinna and Dunstan, 1984), and will only be summarized here. The in-phase FRS gives the integral of the lifetime distribution, between the limits $\tau \propto (2\pi\omega)^{-1}$ and ∞, while the in-quadrature FRS gives the lifetime distribution directly. This in-quadrature form of FRS, thus, provides the bulk of our lifetime measurements. For a system with a single characteristics lifetime τ, the in-quadrature FRS spectrum is a symmetric band, of half width 0.7 decades peaked at the frequency

$$f_p = \frac{1}{2\pi\tau} \tag{1}$$

According to Depinna and Dunstan (1984), the lock-in output from all lifetimes components as the frequency is swept is given by

$$S(\omega) = \int_0^\infty P(\tau)s(\omega,\tau)d\tau \tag{2}$$

where $P(\tau)$ is the lifetime distribution, and $s(\omega,\tau)$ is the response function. For quadrature the lock-in response function is given by

$$s(\omega,\tau) = \frac{g_r}{\omega\tau + \frac{1}{\omega\tau}} \tag{3}$$

while in-phase FRS, it takes the following form

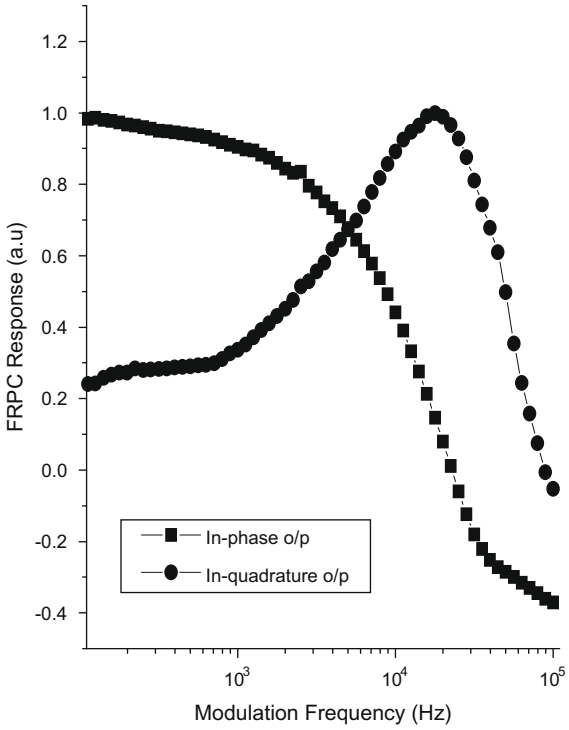

Fig. 1. Frequency-resolved photocurrent (FRPC) response function for the in-phase and in-quadrature of a-Se with a single well defined lifetime at room temperature.

$$s(\omega,\tau) = \frac{g_r}{1+\omega^2\tau^2} \tag{4}$$

where g_r is the excitation rate. For comparison, the in-phase and quadrature response functions of a-Se used are represented together in Fig. 1. Although the in-quadrature FRS is the most useful form, the in-phase version can also give important additional information on the existence of fast processes beyond the time domain of the in-quadrature measurements.

It is worth remembering that if one knows the quadrature response from $\omega = 0 \rightarrow \infty$ (which one does not), a Kramers–Kronig transform will give the in-phase response. That is all the information is in either response, if complete in ω.

4. Results and discussion

In-quadrature ($\phi = 90^\circ$) frequency-resolved photocurrent (FRPC) responses of a-Se thin films in the frequency interval between 10 Hz and 100 kHz were measured as a function of the temperature, excitation wavelength and applied electric field (d.c.). Since the energy of the excitation light is much higher than the optical band gap of this material, we assume that the carriers are photo-excited between extended states and then a trap limited recombination occurs.

Fig. 2 shows the FRPC response at various applied electric fields. The light intensity (632.8 nm, from HeNe laser) and temperature were kept constant at 2.31 mW ($\approx 2.3 \times 10^{19}$ photons $cm^{-2}\,s^{-1}$) and room temperature

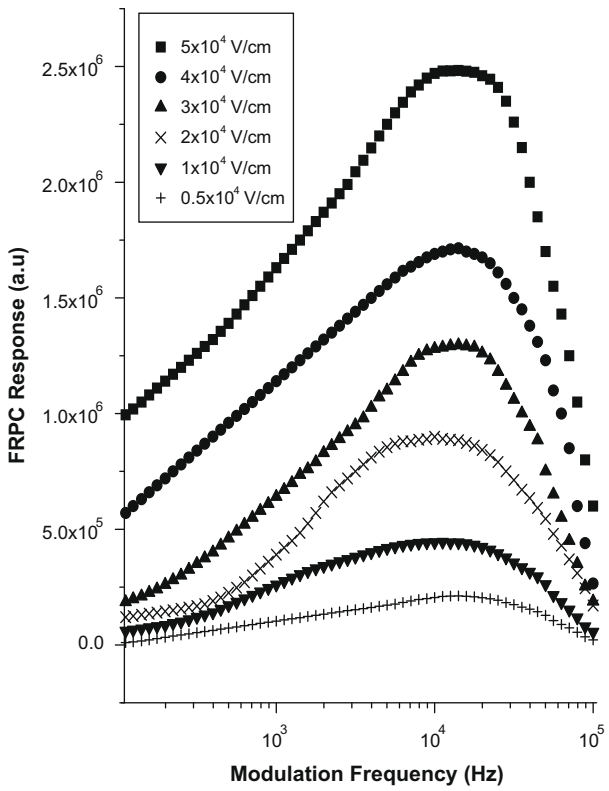

Fig. 2. FRPC response of a-Se thin films under various applied electric fields. Excitation light intensity is 2.31 mW with the wavelength of 632.8 nm. Data were taken at room temperature (297 K).

(297 K) respectively during measurements. As seen, there is only a single and broad distribution peaked at around 14,125 Hz.

As mentioned previous section, the experimental techniques of time-resolved spectroscopy (TRS) and frequency-resolved spectroscopy (FRS) have quite commonly been used for measurements of the lifetime distribution (Fuhs, 2008). While TRS records the photoluminescence decay as response to a short laser pulse excitation, FRS measures the 90°-phase-shifted frequency response under stationary excitation conditions and therefore often the term of quadrature frequency-resolved spectra (QFRS) is used. An advantage of the latter method is that the QFRS signal intensity directly yields the distribution function of the logarithm of lifetimes. Although equivalent in theory, these two methods led to conflicting results. Based on TRS data the geminate-pair model was developed (Tsang and Street, 1979) according to which the recombining electron–hole pairs are correlated, being created in the same absorption process. The QFRS data, however, seemed to indicate that there is no such correlation, which led to the distant-pair model, which proposes that electrons and holes are randomly distributed in space and recombine non-geminately (Dunstan, 1982). This discrepancy was finally resolved when it was demonstrated that geminate recombination is observable in QFRS once the generation rate is decreased below a critical value of about $G_C \approx 5 \times 10^{18}$ cm^{-3} s^{-1} (Bort et al., 1991). Actually, the radiative-tunneling model predicts the existence of two recombination regimes with different recombination kinetics. In the geminate-pair model it is assumed that diffusion during thermalization does not separate the photo-excited electrons and holes such that recombination occurs between electron–hole pairs that have been created in the same absorption event. In the distant-pair model it is supposed that the carriers are able to diffuse apart and recombine radiatively with the nearest available partner in a non-geminate process. Hence, when the generation rate G increases, there should be a transition from geminate to non-geminate recombination connected with a change in the kinetics: At low G the lifetime distribution of geminate pairs is independent of the generation rate, whereas at high G the lifetime distributions is expected to shift to shorter times with increasing G due to the strong decrease of the lifetime with increasing carrier concentration (Fuhs, 2008).

The frequency-resolved spectroscopy methods were developed for interpreting photoluminescence measurements. It can also be used to analyse modulated photoconductivity data. While photoluminescence reflects the (radiative) recombination of photo-excited carriers, photoconductivity reflects the transport of those carriers that do not recombine.

FRS has been widely applied to the study of lifetime and recombination processes (Depinna and Dunstan, 1984; Schubert et al., 1996; Ogihara et al., 1996; Oheda, 1995). According to FRS method, the in-phase and quadrature photoluminescence response in amorphous materials have been treated in detail. This treatment has been applied to frequency-resolved photocurrent (FRPC) response in amorphous materials (Wagner et al., 1984; Searle et al., 1987; Main et al., 1991; Kaplan, 2005).

Using Eq. (1), from Fig. 2 the lifetime of ~11.3 μs was calculated for all curves. As seen, the applied electric field has no important effects on lifetime distributions except for FRPC magnitude. This results was also valid at low temperatures measured.

Fig. 3 shows the temperature dependences of lifetime for the excitation intensity of 2.3 mW (632.8 nm). Now the applied electric field was kept constant at 5×10^4 V/cm. Obviously a second peak appears at the low temperature of 25 K. It peaked at around 1000 Hz, which corresponds to a lifetime of 159.2 μs. This result provides a way of distinguishing between capture and recombination rates. If the carriers move in extended states, and detrapping is not important, then only one peak is expected in the quadrature FRPC, corresponding to the total capture rate into localized levels. At higher temperatures, the carriers may be thermally ionised from recombination or trapping states. Simple models indicate that a second lifetime proportional to the detrapping rate will be seen even if only one recombination path is present. However, because the release rate is thermally activated both the second lifetime and the strength of its contribution will be strongly temperature dependent (Searle et al., 1987; Ambros et al., 1991).

Fig. 4 shows the FRPC response vs $1000/T$ under various applied electric fields. The excitation intensity

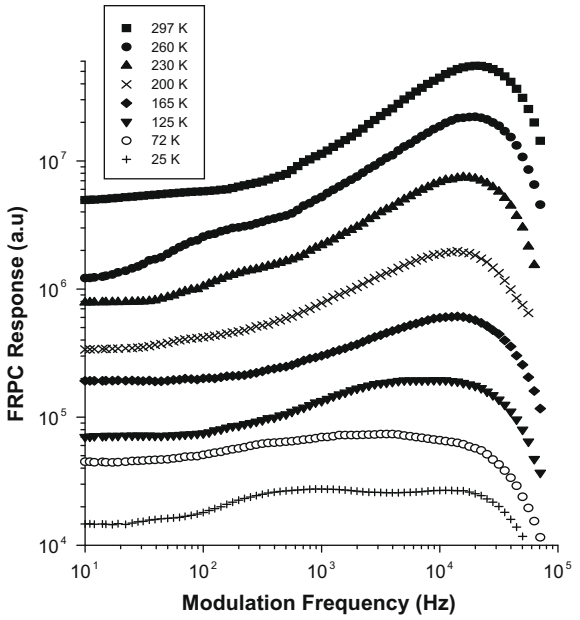

Fig. 3. FRPC response of a-Se thin films at various temperatures. Excitation light intensity is 2.31 mW with the wavelength of 632.8 nm.

(632.8 nm) and the modulation frequency were kept constant at 2.31 mW and 1 kHz respectively. As can be seen, there exists three regions for the temperature dependence of FRPC response: (i) at low temperature (below 60 K) FRPC response is nearly constant and proportional to applied electric field. The low temperature FRPC response can be associated with hopping in the band-tail (Hoheisel et al., 1984; Johanson et al., 1989). The theory of hopping photoconductivity (Shklovskii et al., 1982) suggests that at low temperature ($T = 0$ K approach) photo-excited carriers can only hop down in energy through the localized band-tail states before they recombine. Only those carriers which escape geminate recombination contribute to the photoconductivity; (ii) at intermediate temperatures ($60\ \text{K} < T < 100\ \text{K}$) FRPC response is enhanced with T. (iii) at high temperatures (above 100 K) the magnitude of FRPC and the kinetics are determined by the Fermi level position and the density of occupancy of localized gap states. In other words, the transport occurs in the extended states and the carrier lifetime is controlled as in crystalline photoconductors by multiple trapping model, the occupancy and capture cross-sections of the deep gap states which act as recombination centers. At high temperature region, the FRPC response increases almost linearly with increasing temperatures. It produced by the thermal activation of photocarriers, follows the exponential relation,

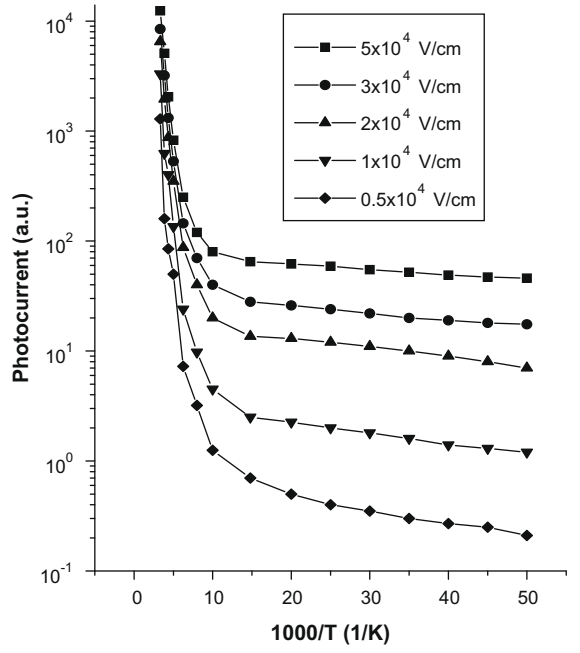

Fig. 4. Frequency-resolved FRPC response vs $1/T$ for a-Se thin films under various applied electric fields. Excitation light intensity was kept constant at 2.31 mW with the wavelength of 632.8 nm. The modulation frequency is 1 kHz. The lines are here as guide to the eye.

$$I_{ph} = I_0 \exp\left(\frac{-E_a}{kT}\right) \tag{5}$$

where I_0 is a pre-factor, k is the Boltzmann's constant, and E_a is the activation energy. An average value of $E_a = 147 \pm 35$ meV was determined. It does not depend on the applied electric fields. Our result for E_a is in agreement with the d.c. photocurrent results (Nesheva, 1996). In order to explain this low value of the activation energy, one can assume that the hole transport in a-Se thin films is probably controlled by the valence band-tail states.

The main interest for the kinetics of carrier recombination in chalcogenide glasses is the dependence of photocurrent I_{ph} on the photogeneration rate G:

$$I_{ph} \propto G^{v} \tag{6}$$

The exponent v is defined by

$$v = \frac{d[\ln(I_{ph})]}{d[\ln(G)]} \tag{7}$$

It is now well known that the value of the exponent v differs in various chalcogenide materials. In most cases, a sublinear dependence is found and the exponent v in this power-law relation has quite complicated variations with temperature, excitation light intensity and wavelength, and applied electric field (Kaplan, 2005; Rose, 1978; Sahin and Kaplan, 2006).

Fig. 5 shows the excitation light intensity dependence of FRPC for six applied electric fields determined at a constant modulation frequency of 10 Hz and at a temperature of 290 K. Obviously, there is a minor increase in the exponent v with decreasing applied electric fields due to dominated recombination effect at low fields.

Fig. 6 shows the same dependence for different wavelengths at the modulation frequency of 100 Hz. The data were taken at room temperature (290 K) and the applied electric field was kept constant at 5×10^4 V/cm. Clearly, v increases with increasing wavelengths, and reaches a maximum value of 0.78 at around 514.5 nm, and then it decreases

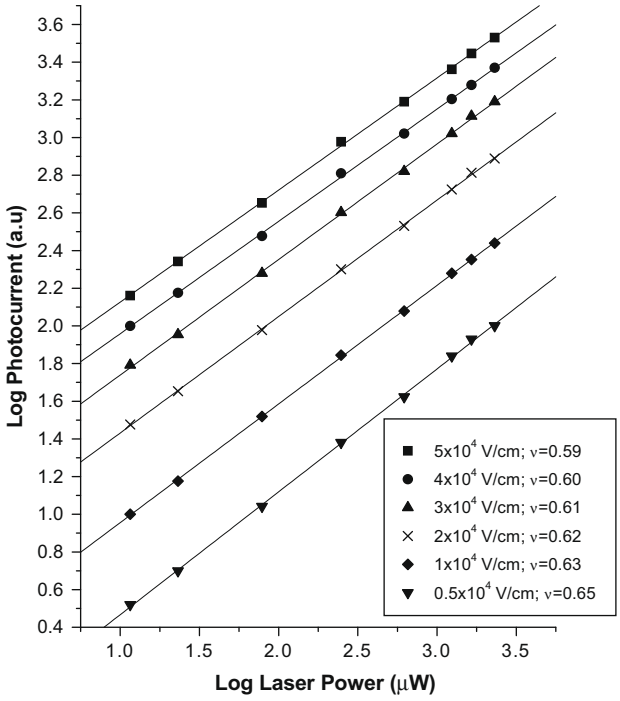

Fig. 5. Excitation light intensity dependence of FRPC response of a-Se thin films at various applied electric fields. Data were taken at 297 K and 10 Hz.

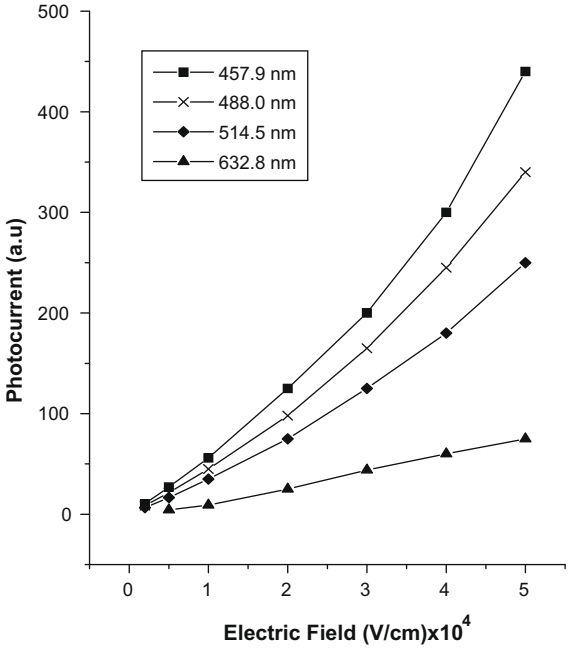

Fig. 7. Electric field dependence of FRPC response of a-Se thin films for different excitation wavelengths. Excitation light intensity was kept constant at 1.2 mW for all wavelengths. Data were taken at 297 K and 10 Hz. The lines are here as guide to the eye.

with increasing wavelengths. Rose (1978) suggests that $v = 1$ corresponds to monomolecular recombination and $v = 0.5$ to bimolecular recombination. However, in the case of continuous distribution of traps the value of v may be anywhere between 0.5 and 1.0 depending on the intensity and the temperature range. As can be seen from Figs. 5 and 6, the values of exponent v lie between 0.50 and 0.78 depending on applied electric fields and excitation wavelengths. These results indicate the presence of a continuous distribution of localized states in the energy gap.

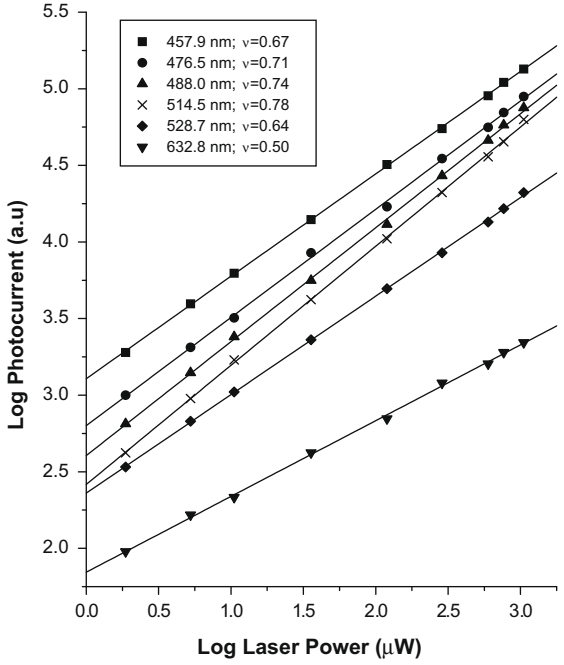

Fig. 6. Excitation light intensity dependence of FRPC response of a-Se thin films for different excitation wavelengths. Data were taken at 297 K and 100 Hz. The applied electric field was 5×10^4 V/cm.

Fig. 7 shows the electric field dependence of FRPC response at different excitation wavelengths. The intensity of excitation light was kept constant at around 1.2 mW for all wavelengths. Data were taken at 290 K and at 10 Hz. We must report that I–V (current–voltage) measurement taken in the dark proved that the contacts (Au or Al) deposited on a-Se were perfectly ohmic. The dark conductivity of a-Se was found to be around 10^{-12} ohm^{-1} cm^{-1} at 290 K. From Fig. 7, it is obvious that the current–voltage relation is not linear at high applied fields ($>2 \times 10^4$ V/cm) and at low wavelengths (<514.5 nm) under the illumination.

In the case of the space charge limited current (Petretis and Balciuniene, 2002), the deep centers of the charge transfer generation become deep trapping centers. So, when the energy spectrum of deep centers changes the positions of characteristics break points of the current dependence on the voltage must change, because these points are caused by the mechanism of the charge transfer. When the value of the voltage reaches a critical point voltage, the deep localized states recharge under the influence of the electric field and the quasi-Fermi level moves to a new energetic position. With the increase of illumination and thus absorption, the concentration of injected carriers increases, and the influence of recharge of deep levels manifest itself only when the external electric field is stronger. It should be pointed out that the light in the region of the electrode

forms a reservoir not only of main carriers (holes) of the current but of the electrons as well. Since the electrons in a-Se are less mobile as compared with holes, they are trapped into deep states and have an influence on the recharge of states and can cause inhomogeneous distribution of the field in the area near the electrodes.

5. Conclusion

The modulated (10 Hz to 100 kHz) photocurrent responses of a-Se thin film samples were measured as a function of temperature, excitation wavelength of light intensity, and applied electric fields. From the quadrature o/p of the lock-in amplifier, we observed that modulated photocurrent response shows a single broad peak distribution at room temperature, and its peak frequency (14125 Hz) and thus its corresponding lifetime (11.3 μs) is found to be almost independent of applied electric field and temperature. However, at the very low temperature measured (25 K), a second peak was discovered in the QFRS at low frequency range, in addition to the room temperature result. Its lifetime was found to be 159.2 μs, which can be related to detrapping rate.

At high temperatures, the FRPC vs $1/T$ curves at various applied electric fields show an activated behaviour with a small activation energy value of 147 ± 35 meV for an excitation intensity of 2.31 mW. We explained that the hole transport in a-Se thin films is probably controlled by the valence band-tail states.

The effects of applied electric field and excitation wavelength on the exponent $v(I_{ph} \propto G^{v})$ were investigated. Its values were determined in the range $v \cong 0.59$–0.65 for different applied electric fields, and $v = 0.50$–0.78 for different wavelengths of excitation light. This suggests that in a-Se thin film the quasi-Fermi level is shifting in a more or less exponential distribution of localized states.

The effects of excitation wavelength and temperature on the current–voltage (I–V) measurements were also studied. The results show that a very little non-ohmic contact behaviour at high applied electric fields ($>2 \times 10^4$ V/cm) and at low wavelengths (<514.5 nm). This is confirmed at all temperatures measured.

Acknowledgements

The author is grateful to Dr. T.M. Searle for helpful discussions. This work was supported under Mersin University contract no. BAP-EF OFMA (RK) 2006-2.

References

Acevedo, A.M., 2009. Variable band-gap semiconductors as the basis of new solar cells. Sol. Energy 83, 1466.

Ambros, S., Carius, R., Wagner, H., 1991. Lifetime distribution in a-Si:H: geminate-, non-geminate-, and Auger-processes. J. Non-Cryst. Solids 137–138, 555.

Bhattacharya, R.N., Ramanathan, K., 2004. Cu(In, Ga)Se_2 thin film solar cells with buffer layer alternative to CdS. Sol. Energy 77, 679.

Bindu, K., Lakshmi, M., Bini, S., Sudha Kartha, C., Vijayakumar, K.P., Abe, T., Kashiwaba, Y., 2002. Amorphous selenium thin films prepared using chemical bath deposition: optimization of the deposition process and characterization. Semicond. Sci. Tech. 17, 270.

Bort, M., Fuhs, W., Liedtke, S., Strachowitz, R., 1991. Geminate recombination in a-Si:H. Philos. Mag. Lett. 64, 227.

Dahson, A., Amer, H.H., Moharam, A.H., Othman, A.A., 2006. Photoconductivity of amorphous As-Se-Sb thin films. Thin Solid Films 513, 369.

Depinna, S.D., Dunstan, D.J., 1984. Frequency-resolved spectroscopy and its application to the analysis of recombination in semiconductors. Philos. Mag. B 50, 579.

Dunstan, D.J., 1982. Kinetics of distant-pair recombination. 1. Amorphous silicon luminescence at low temperature. Philos. Mag. B 46, 579.

Emelianova, E.V., Qamhieh, N., Brinza, M., Adriaenssens, G.J., Kasap, S.O., Johanson, R.E., Arkhipov, V.I., 2003. Defect levels and charge carrier photogeneration in amorphous selenium layers. J. Non-Cryst. Solids 326–327, 215.

Fuhs, W., 2008. Recombination and transport through localized states in hydrogenated amorphous and microcrystalline silicon. J. Non-Cryst. Solids 354, 2067.

Green, M.A., 2003. Crystalline and thin-film silicon solar cells: state of the art and future potential. Sol. Energy 74, 181.

Green, M.A., 2004. Recent developments in photovoltaics. Sol. Energy 76, 3.

Gorley, P.M., Khomyak, V.V., Vorobiev, Y.V., Hernandez, J.G., Horley, P.P., Galochkina, O.O., 2008. Electron properties of n- and p-$CuInSe_2$. Sol. Energy 82, 100.

Goswami, D.Y., Vijayaraghavan, S., Lu, S., Tamm, G., 2004. New and emerging developments in solar energy. Sol. Energy 76, 33.

Hayashi, K., Mitsuishi, N., 2002. Thickness effect of the photodarkening in amorphous and chalcogenide films. J. Non-Cryst. Solids 299–302, 949.

Hoheisel, M., Carius, R., Fuhs, W., 1984. Photoconductivity and photoluminescence of a-Si:H at low temperature. J. Non-Cryst. Solids 63, 313.

Johanson, R.E., Fritzsche, H., Vomvas, A., 1989. Universal behavior of the normalised photoconductivity at low temperatures in amorphous semiconductors. J. Non-Cryst. Solids 114, 274.

Joraid, A.A., Alamri, S.N., Abu-Sehly, A.A., 2008. Model-free method for analysis of non-isothermal kinetics of a bulk sample of selenium. J. Non-Cryst. Solids 354, 3380.

Kaplan, R., 1993. Optically modulated photoconductivity studies of amorphous semiconductors. Ph.D. Thesis. University of Sheffield, UK.

Kaplan, R., 2005. Comparative frequency-resolved photoconductivity studies of amorphous semiconductors. Sol. Energy Mater. Sol. Cells 85, 545.

Kessler, F., Rudmann, D., 2004. Technological aspects of flexible CIGS solar cells and modules. Sol. Energy 77, 685.

Kolobov, A.V., Tanaka, K., 2001. In: Nalwa, H.S. (Ed.), . In: Handbook of Advanced Electronic and Photonic Materials and Devices, vol. 5. Academic Press, New York, p. 47.

Lee, S.H., 2009. Cost effective process for high-efficiency solar cells. Sol. Energy 83, 1285.

Li, W., Sun, Y., Liu, W., Zhou, L., 2006. Fabrication of Cu(In, Ga)Se_2 thin films solar cell by selenization process with Se vapor. Sol. Energy 80, 191.

Lyubin, V., Klebanov, M., Tikhomirov, V.K., 2002. Photoinduced anisotrophy of photoconductivity in chalcogenide amorphous films. J. Non-Cryst. Solids 299–302, 945.

Main, C., Webb, D.P., Bruggemann, R., Reynolds, S., 1991. Modulated and transient photoconductivity in a-As_2Se_3. J. Non-Cryst. Solids 137–138, 951.

Mellor, A., Domenech, J.L.G., Chemisana, D., Rosell, J.I., 2009. A two-dimensional finite element model of front surface current flow in cells under non-uniform, concentrated illumination. Sol. Energy 83, 1459.

Murugvel, S., Asokan, S., 2002. Composition dependence of photoconductivity of $Al_{20}As_xTe_{80-x}$ glasses. J. Non-Cryst. Solids 303, 296.

Nesheva, D., 1996. Photoconductivity and recombination in amorphous Se/CdSe multilayers. Thin Solid Films 280, 51.

Ogihara, C., Ishimura, H., Kinoshita, T., Ikeda, K., Morigaki, K., 1996. Distribution of lifetime of photoluminescence in band-edge modulated a-$Si_{1-x}N_x$:H films. J. Non-Cryst. Solids 198–200, 255.

Oheda, H., 1995. Photoluminescence mechanism in hydrogenated amorphous silicon studied by frequency-resolved spectroscopy. Phys. Rev. B 52, 16530.

Pawar, S.M., Moholkar, A.V., Suryavanshi, U.V., Rajpure, K.Y., Bhosale, C.H., 2007. Electrosynthesis and characterization of iron selenide thin films. Sol. Energy Mater. Sol. Cells 91, 560.

Petretis, Br., Balciuniene, M., 1998. Photoexcited recharge of localized states in amorphous selenium. J. Non-Cryst. Solids 226, 294.

Petretis, Br., Balciuniene, M., 2002. Negative photoconductivity of illuminated a-Se layers. J. Non-Cryst. Solids 311, 42.

Rose, A., 1978. Concepts in Photoconductivity and Allied Problems. Krieger, New York, p. 38.

Sahin, M., Kaplan, R., 2006. Intensity and temperature dependence of photocurrent of a-Si:H Schottky diodes. Curr. Appl. Phys. 6, 114.

Schubert, M., Stachowitz, R., Fuhs, W., 1996. Geminate and non-geminate recombination in amorphous silicon (a-Si:H). J. Non-Cryst. Solids 198–200, 251.

Searle, T.M., Hopkinson, M., Edmeads, M., Kalem, S., Austin, I.G., Gibson, R.A., 1987. Recombination in a-Si:H based materials: evidence for two slow radiative processes. In: Kastner, M.A., Thomas, G.A., Ovshinsky, S.R. (Eds.), Disordered Semiconductors. Plenum, New York, p. 357.

Searle, T.M., 1991. Optical properties of disordered electronic materials. In: Kirov, N. (Ed.), New Physical Problems in Electronic Materials. World Scientific, Singapore, p. 118.

Sharma, I., Tripathi, S.K., Monga, A., Barman, P.B., 2008. Electrical properties of a-Ge–Se–In thin films. J. Non-Cryst. Solids 354, 3215.

Shirakawa, Y., Harada, S., Shimosaka, A., Hidaka, J., Kusakabe, M., 2002. Interfacial effect on electronic conductivities in amorphous selenium systems. J. Non-Cryst. Solids 312–314, 327.

Shklovskii, B.I., Fritzsche, H., Baronovskii, S.D., 1982. Electronic transport and recombination in amorphous semiconductors at low temperatures. Phys. Rev. Lett. 62, 2989.

Thakur, A., Sharma, V., Chandel, P.S., Goyal, N., Saini, G.S.S., Tripathi, K., 2006. Photoconductivity in thin film of a-$(Ge_{20}Se_{80})_{0.90}Sn_{0.10}$. Mater. Sci. 41, 2327.

Tsang, C., Street, R.A., 1979. Recombination in plasma-deposited amorphous Si:H. Luminescence decay. Phys. Rev. B 19, 3027.

Venkatachalam, M., Kannan, M.D., Muthukumarasamy, N., Prasanna, S., Jayakumar, S., Balasundaraprabhu, R., Saroja, M., 2009. Investigation on electron beam evaporated $Cu(In_{0.85}Ga_{0.15})Se_2$ thin film solar cells. Sol. Energy 83, 1652.

Wagner, D., Irsigler, P., Dunstan, D.J., 1984. Photoconductivity measurements in a-Si:H by frequency-resolved spectroscopy. J. Phys. C: Solid State Phys. 17, 6793.

Waldau, A.J., 2004. Status of thin film solar cells in research, production and the market. Sol. Energy 77, 667.

Zhang, X., Drabold, D.A., 1998. Evidence for valence alternation, and a new structural model of amorphous selenium. J. Non-Cryst. Solids 241, 195.